Efficient Malaria Parasite Detection From Diverse Images of Thick Blood Smears for Cross-Regional Model Accuracy

Yuming Zhong, Ying Dan, Yin Cai, Jiamin Lin, Xiaoyao Huang, Omnia Mahmoud, Eric S. Hald, Akshay Kumar, Qiang Fang, and Seedahmed S. Mahmoud, *Senior Member, IEEE*

***Abstract*—*Goal*: The purpose of this work is to improve malaria diagnosis efficiency by integrating smartphones with microscopes. This integration involves image acquisition and algorithmic detection of malaria parasites in various thick blood smear (TBS) datasets sourced from different global regions, including low-quality images from Sub-Saharan Africa. *Methods:* This approach combines image segmentation and a convolutional neural network (CNN) to distinguish between white blood cells, artifacts, and malaria parasites. A portable system integrates a microscope with a graphical user interface to facilitate rapid malaria detection from smartphone images. We trained the CNN model using open-source data from the Chittagong Medical College Hospital, Bangladesh. *Results:* The validation process, using microscopic TBS from both the training dataset and an additional dataset from Sub-Saharan Africa, demonstrated that the proposed model achieved an accuracy of 97.74% $\pm$ 0.05% and an F1-score of 97.75% $\pm$ 0.04%. Remarkably, our proposed model with AlexNet surpasses the reported literature performance of 96.32%. *Conclusions:* This algorithm shows promise in aiding malaria-stricken regions, especially those with limited resources.**

***Index Terms*—Computer-aided diagnosis, image segmentation, malaria parasites, microscope, neural networks, smartphones.**

Manuscript received 5 September 2023; revised 22 October 2023 and 23 October 2023; accepted 24 October 2023. Date of publication 30 October 2023; date of current version 23 November 2023. This work was supported by the Li Ka Shing Foundation Cross-Disciplinary Research under Grant 2020LKSFG04C. The review of this article was arranged by Editor Yasemin M. Akay. *(Corresponding author: Seedahmed S. Mahmoud.)*

Yuming Zhong, Ying Dan, Yin Cai, Jiamin Lin, Eric S. Hald, Akshay Kumar, Qiang Fang, and Seedahmed S. Mahmoud are with the Department of Biomedical Engineering, College of Engineering, Shantou University, Shantou 515063, China, and also with the The Frontier Technology Research Institute, First Affiliated Hospital of Shantou University, Shantou 515063, China (e-mail: 20ymzhong@stu.edu.cn; yingdan223@gmail.com; 20ycai@stu.edu.cn; 20jmlin@stu.edu.cn; hald@stu.edu.cn; akksh@outlook.com; qiangfang@stu.edu.cn; mahmoud@stu.edu.cn).

Xiaoyao Huang is with Shantou University Medical College, Shantou University, Shantou 515063, China (e-mail: xiaoyaohuang3@gmail.com).

Omnia Mahmoud is with Alkawa Hospital, Alkawa 28815, Sudan (e-mail: mam0910408891@gmail.com).

This article has supplementary downloadable material available at https://doi.org/10.1109/OJEMB.2023.3328435, provided by the authors.

Digital Object Identifier 10.1109/OJEMB.2023.3328435

***Impact Statement*—The project aims to enable rapid malaria detection in resource-limited settings by building a portable microscope and a smartphone with deep learning models.**

I. Introduction

MALARIA is a potentially life-threatening disease transmitted by infected female Anopheles mosquitoes. According to the World Malaria Report 2021 [1], there were approximately 241 million cases in 2020, with an estimated 627,000 deaths, marking a substantial increase from 2019. Notably, malaria is endemic in 85 countries, especially in sub-Saharan Africa, where medical resources are limited [1], [2], [3]. Early and accurate diagnosis is an important cornerstone in controlling transmission and preventing deaths.

Conventional malaria diagnosis relies on two primary methods: light microscopy and immunochromatographic rapid diagnostic tests (RDTs) [4]. However, the gold standard for malaria diagnosis, especially in resource-poor settings, involves the examination of Giemsa-stained thick and thin blood films under a conventional light microscope at a magnification of 1000X [2], [3], [5]. This labour-intensive method demands skilled microscopists for manual counting of parasites and white blood cells (WBCs) [4], [6], [7]. Malaria infections are typically reported as the percentage of infected red blood cells (RBCs) per 100 RBCs counted or as the number of parasites per microliter of blood, calculated based on parasite counts per 100 WBCs on a smear [5]. Thick blood smears (TBS) and thin blood smears are the two types of peripheral blood smears commonly used [8]. TBS, which increases the density of red blood cells on the slide, offers higher sensitivity for detecting malarial infections [7], [9]. Although effective, manual examination of microscopy is time-consuming and laborious. Additionally, in resource-constrained settings, precise WBC counts are often approximated, making the management of malaria less effective [10]. Hence, there is an urgent need for a rapid and affordable malaria detection system.

The recent advancements in CNN for object detection in natural images have the potential to revolutionize malaria diagnosis [11], [12]. Automated systems can significantly enhance diagnostic accuracy and reduce costs. However, existing methods rarely focus on low-quality data from Africa and often do not include WBC counts in their assessments of malaria parasite density [6], [13], [14], [15].

Therefore, we present a novel method that utilizes deep learning to accurately detect malaria parasites and count WBCs. We address the issue of image distortion caused by mobile phone optical interfaces to exploit the widespread use of smartphones for capturing microscope images [16]. Our contributions can be summarized as follows:

1) Generalized algorithm development: we devised a versatile algorithm capable of detecting malaria parasites and counting WBCs in diverse TBS film datasets from Asia and Sub-Saharan Africa.
2) Resolution of blurred image problem: we developed an algorithm to tackle blurred images resulting from the interface between mobile phone optics and microscopes.
3) Optimization with low-quality images: our model was optimized using low-quality images from Sudan in Sub-Saharan Africa, ensuring its applicability in resource-limited areas.
4) Portable malaria detection system: we created a portable system integrating a microscope with a smartphone featuring a user-friendly interface.
5) Automatic parasite concentration assessment: our system automatically assesses malaria parasite concentration in both thick and thin blood smears, displayed in the graphical user interface (GUI).

This paper is organized as follows: in Section II, we present related research on the automatic detection of malaria parasites. In Section III, we discuss the proposed algorithm and methods. In Section IV, we present our validation results and a discussion of our findings. In Section V, we emphasize our conclusions and future work required for efficient malaria parasites detection.

II. Related Work

Microscopic image-based automatic detection of malaria parasites from TBS involves a sequence of processes: image acquisition, preprocessing, and classification [17]. In most studies, automatic detection is performed on light microscopy images because light microscopy is widely used for malaria diagnosis in resource-restricted regions [7]. Currently, the segmentation of WBCs in thin blood smears using color gamut space, combined with deep learning techniques for classifying and counting WBCs, has been extensively researched across various diseases, yielding significant and promising results [18], [19], [20]. Our study focuses on preprocessing techniques aimed at eliminating redundant details, such as WBCs and artifacts, from the acquired images. To enhance the accuracy of malaria parasite detection and adhere to the parasite density criterion [21], [22], which necessitates the calculation of WBCs, our automatic detection model incorporates WBC segmentation, counting, and artifact removal. Consequently, our approach facilitates malaria detection utilizing TBS images.

A. Methods of Segmentation to Detect WBC

Several studies have been conducted to segment WBCs and remove artifacts from microscopic blood smears [23], [24], [25]. Kaewkamnerd et al. initially employed an adaptive threshold (Otsu) method to extract artifacts in TBS [26]. Elter et al. used black hat morphological operation separation of WBCs and platelets [27]. Delahunt et al. used Otsu to extract leukocytes and classified them with SVM, achieving a specificity of 72.1% [28]. Feng Yang et al. extracted leukocytes in combination with Otsu and morphological manipulations [13]. Manescu et al. used RetinaNet to detect leukocytes and achieved an AUC of 96% [14]. In their study, Olayah et al. proposed a method for classifying WBC types. They achieved this by using an average value filter to enhance the image and employing a hybrid model based on CNN and manual features. This approach yielded an impressive accuracy rate of 99.8% [20]. Ghosh et al. employed gradient-based region growing with neighbourhood influence to achieve a more accurate recovery of region boundaries and classification of WBCs. This method was applied after segmenting the WBCs using background scaling and other techniques. The sensitivity and specificity were 96.4% and 79.6%, respectively [19]. Acharya et al. utilized the K-medoids method to identify leukocyte nuclei in thin blood smears and introduced a novel technique for extracting leukocyte cytoplasm from various abnormal cells. This method achieved a discrimination rate of 99.81% for both RBCs and WBCs [18].

Previous studies have endeavoured to differentiate malaria parasites from stained WBCs. However, these studies frequently neglected specific challenges, such as the overlap of WBCs, a phenomenon known as cytoadherence. This oversight has resulted in inaccuracies in cell counting. Additionally, existing literature [13], [14], [23], [24], [25], [26], [27], [28], [29] mainly focuses on WBCs identification in TBS, neglecting quantification. In existing research studies [18], [19], the focus is primarily on the WBC count in thin blood smears, coupled with the analysis of WBC cytoplasm and nucleus division. However, the morphology of WBCs is considerably more intricate, and the cytoplasm is not clearly visible in TBS. Consequently, the method used for WBC counting in thin blood smears cannot be applied to TBS due to the lack of distinct cytoplasmic features. Our research addresses these issues by combining colour per intensity and morphological characteristics to accurately segment and count WBCs, improving the accuracy of cell counting in this context.

B. Methods of Detecting Parasites

Three widely used approaches for automatically detecting malaria parasites are image processing, classical machine learning, and deep learning (DL) [30], [31], [32]. DL has become increasingly popular in a wide range of applications within the health sector, including the analysis of medical images [29]. It has become increasingly popular in a wide range of applications within the health sector, including the analysis of medical images.

In the last three years, DL has emerged as a viable approach for detecting malaria parasites in microscopic images. Fetulhak et al. used the modified YOLOV4 model to achieve an average accuracy of 96.32% [15]. Manescu et al. built a DeepMCNN model based on VGG19 with 92% sensitivity and 90% specificity [14]. Rose Nakasi et al. combined Faster R-CNN and SSD models. The Faster R-CNN model achieved a mAP of 0.5506

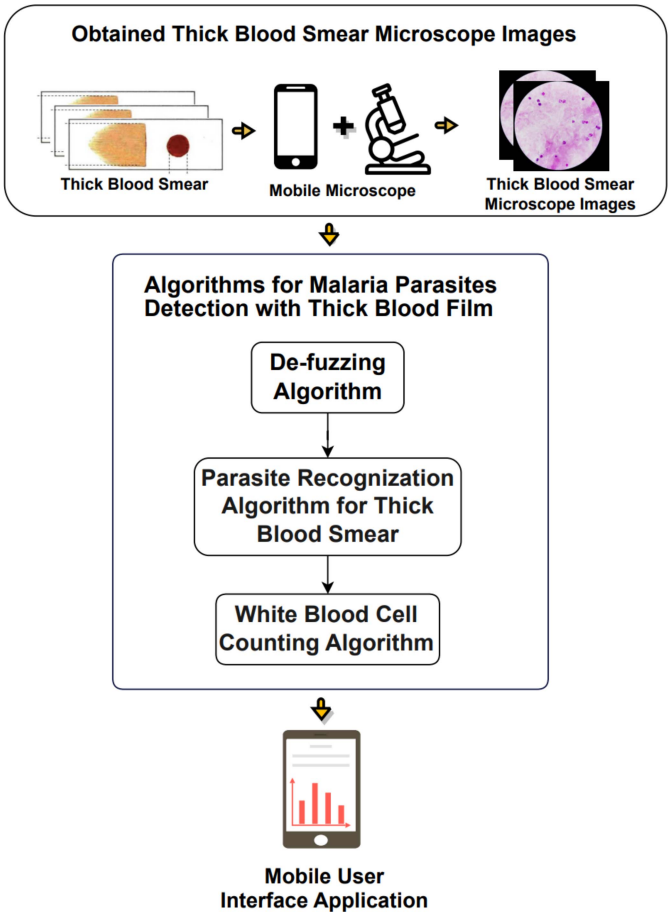

Fig. 1. Proposed portable malaria parasite detection system.

for malaria trophozoite detection alone and a mAP of 0.892 for WBC detection [6]. Yang et al. employed a customized version of VGG19 for Plasmodium classification, achieving a sensitivity of 92.59%, a specificity of 94.25%, and an accuracy of 93.46% [13].

In contrast to previous studies [6], [13], [14], [15] on automatic malaria blood smear detection, our method introduces a multitask approach for detecting malaria parasites and counting WBCs with robustness and high accuracy.

III. Materials and Methods

Fig. 1 shows the proposed portable malaria parasites detection system that incorporates a microscope and a smartphone with a GUI.

A. Mobile Microscope Platform

In this paper, we present a mobile microscope model that incorporates the functionalities of conventional microscopes. This model provides a magnification capability of 1000x and is compatible with smartphones. Fig. 2 illustrates the prototype of the proposed mobile microscope platform, showcasing its design and features.

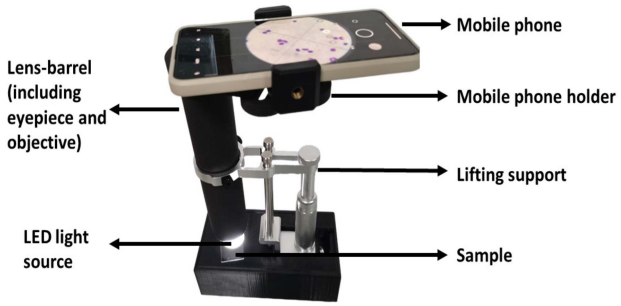

Fig. 2. Prototype of the mobile microscope platform.

To develop this model, we employed FUSION 360 modelling and 3D printing techniques to fabricate the primary components. Subsequently, these components were assembled along with optical elements (a 10x eyepiece and a 100x objective lens), an LED light source, a lifting support, and a mobile phone holder. Specifically, this setup includes a base LED light source capable of automatically adjusting its brightness for brightness correction. This feature ensures that the impact of external illumination changes is negligible. The combination of these elements enables effective imaging with the mobile microscope. The design specifications of the developed system are provided in Table 1 in the Supplementary Materials.

The results of image acquisition using our proposed mobile microscope platform were presented and compared with images captured using a commercial microscope, as shown in Fig. 1 in the Supplementary Materials.

B. Automatic Detection of Malaria Parasites

In this subsection, we present an automatic detection method for malaria parasites in TBS, addressing the pressing need for efficient and accurate diagnostic techniques. The goal of these advancements is to enhance diagnosis and treatment outcomes.

1) Datasets: The datasets used in this study are listed below:

1) Online TBS dataset from the US National Institutes of Health (NIH).
2) An African Sub-Saharan Sudan dataset.

These datasets serve as a valuable resource for studying parasites and healthy samples, facilitating the development and evaluation of robust algorithms for parasite detection and classification.

To generalize and validate the proposed model, a comprehensive dataset was collected from Sub-Saharan Africa, specifically Sudan. This dataset comprises samples from both parasite infected and healthy individuals. Specimens underwent microscope examination at 1000x magnification after staining with Giemsa stain for improved visibility. The Sub-Saharan dataset primarily includes P. falciparum and P. vivax, the region's most prevalent malaria strains. We captured images using a Huawei Nova 3i Android phone, resulting in a malaria parasite dataset of 111 samples. After segmenting the region of interest (ROI) and applying various operations, we obtained 9,759 infected and 9,759 healthy candidates. In this paper, Table 1 presents the details of the NIH and Sudan datasets.

TABLE 1
NIH AND SUDAN DATASET DETAILS

Dataset	Number of Images	Information	Segmentation Size
NIH	4897 infected thick blood smears 1141 healthy thick blood smears	Obtained at Chittagong Medical College Hospital in Bangladesh Malaria Datasheet (nih.gov)	23,398 infected and 23,398 healthy data
Sudan	99 infected thick blood smears 12 healthy thick blood smears	Obtained from Alkawa Hospital, Alkawa, White Nile State, Sudan	9759 infected and 9759 healthy data

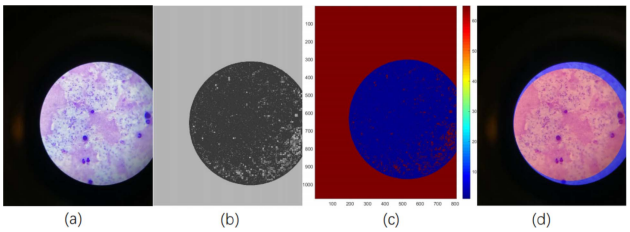

Fig. 3. (a) Images acquired using the proposed mobile phone microscope. (b) Using the blurred image obtained from FIS and the higher grayscale value represents the higher blur in this region. (c) Heat map of the distribution of fuzzy areas. (d) The red area represents the image output from FIS and the blue is the part occluded by the mask.

2) Defuzzing Algorithm: In the image acquisition process, blurred areas may arise due to differences in mobile phone models and varying focal lengths of microscopes. To improve image clarity, we propose a Fuzzy Inference System (FIS) capable of effectively extracting clear areas from the original image. The fuzzy logic approach in image processing entails determining the degree to which a pixel belongs to either an edge or a uniform region [33].

The flowchart and detailed process of the proposed FIS algorithm are presented in Section I-B-1 of the Supplementary Materials. By utilizing the FIS, we can obtain high-quality images, albeit at the cost of sacrificing a portion of the field of view. The application of the FIS algorithm to an image captured by the proposed mobile microscope platform is demonstrated in Fig. 3.

3) Image Segmentation Algorithm:

a) Segmentation of WBCs: The morphology of WBCs varies due to differences in staining time, hemolysis time, and various other factors. These variations present significant challenges to the accuracy of WBC count. Our experiments revealed the challenges associated with effectively adapting to the segmentation and counting of WBCs exhibiting complex morphology, solely relying on adaptive thresholding and morphological operations. To address this challenge, we introduced a two-fold approach. Initially, we transformed the RGB color space into the Lab color space to ensure precise segmentation of the stained images [18], [34]. Subsequently, we combined the *k*-means clustering method with the adaptive threshold technique. This integrated method proved highly effective in segmenting neutrophils and eosinophils, leading to a significant enhancement in the accuracy of WBC counting.

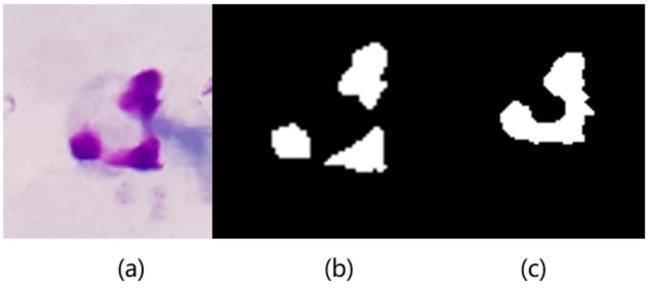

Fig. 4. (a) Eosinophils. (b) The mask obtained using otsu. (c) Use the mask obtained by the proposed method.

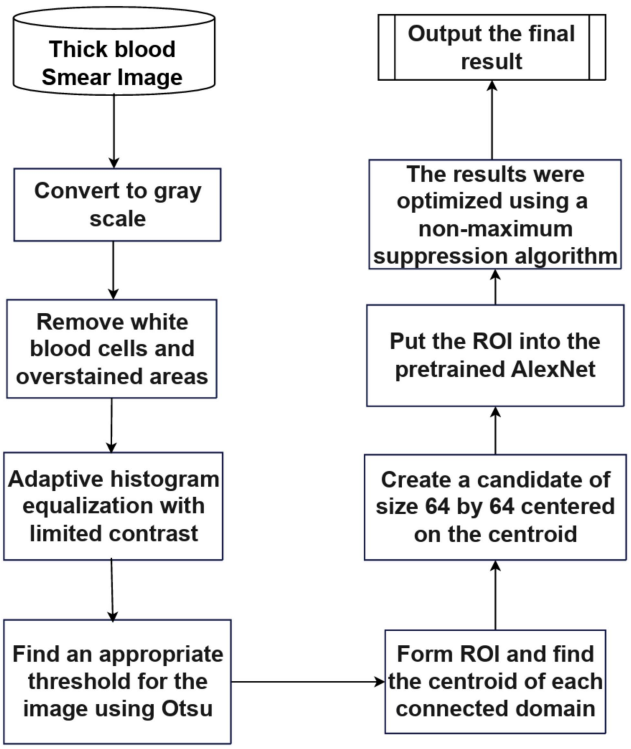

Fig. 5. Flowchart of the proposed parasites segmentation algorithm.

The flowchart and the detailed process of the proposed WBCs segmentation algorithm are shown in Section I-B-2 of the Supplementary Materials. The proposed method accurately segmented the eosinophils, whereas the Otsu method misclassified them, segmenting them as three WBCs. Fig. 4 illustrates the robustness of the proposed method compared to the Otsu method when applied to eosinophils.

b) Parasite candidates' segmentation: The flowchart of the proposed parasites segmentation algorithm is shown in Fig. 5. The WBCs and specific over-stained regions were

removed through morphological manipulation and a WBC detection algorithm. Subsequently, an adaptive histogram equalization method with contrast-limiting properties was applied to enhance the image's contrast. Next, the binary image is generated using Otsu's method [35], an adaptive threshold selection technique designed to determine a binarization threshold. This method simultaneously maximizes the variance within each category while minimizing the variance between the two categories. Based on experimental measurements, it was determined that a matrix size of 64 × 64 was adequate for accommodating the entire malaria parasite. The centroid of all interconnected white domains was computed, and a cropped picture of size 64 × 64 was generated and cantered on the centroid, as a potential candidate for Plasmodium.

4) Deep Neural Network: In recent years, DL algorithms, specifically CNNs, have achieved remarkable classification results in the field of computer vision [36]. Consequently, training such architectures with small datasets, as in the case of this study, presents a challenge and can result in overfitting [37]. Therefore, in this research, transfer learning was employed to train the CNN model. Specific training parameters will be described in Section I-B-3 of the Supplementary Materials.

In our preliminary investigation, we found that VGG and AlexNet outperformed other CNN architectures, such as GoogLeNet and ResNet, in the context of malaria parasite detection. The VGG19 network possesses a deeper hierarchical structure, comprising 19 convolutional and fully connected layers, enabling it to capture higher-level image features. The architecture of the customized AlexNet model for classifying malaria parasites is depicted in Fig. 5 in the Supplementary Materials.

C. Mobile User Interface Application

An efficient and user-friendly graphical user interface (GUI) has been developed to create a rapid and flexible assessment platform for the automatic detection of malaria. Our software enables the intelligent detection of malaria parasites in blood smears, empowering remotely distributed users to create personal profiles and upload test results. This system streamlines doctors' access to diagnostic indicators, thus saving valuable time and reducing labor costs. Additionally, it facilitates the local storage of microscopic images and diagnostic data, contributing to the establishment of a comprehensive patient medical database. Consequently, this conserves valuable medical resources.

The MATLAB APP designer platform was utilized to develop the malaria parasite detection platform, which encompasses several key functions: patient information retrieval, diagnostic results display, manual adjustment, and blood smear mode selection (see Fig. 6). Equations (1) and (2) provide the malaria parasite concentrations for thick and thin blood smears, respectively. The Supplementary Materials, Table 2, provides the degree of infection based on the parasite count in the visual field in TBS.

$$\mathrm{MC}\,(\mu\mathrm{L}) = \frac{P_N{}^{*}8000}{\mathrm{WBC}_N} \tag{1}$$

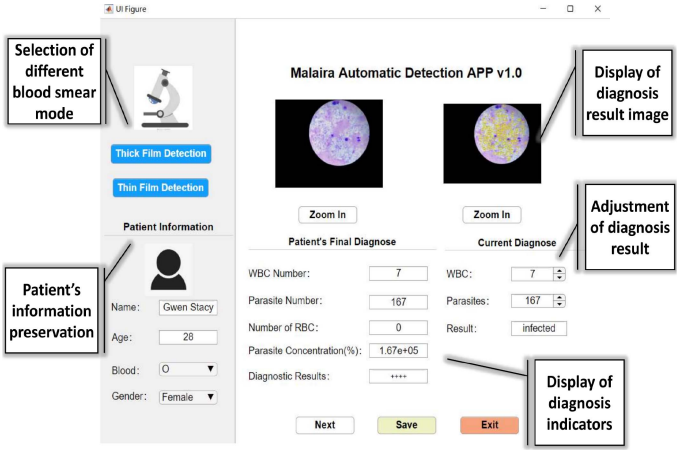

Fig. 6. Malaria parasite detection platform's GUI.

$$\mathrm{MIR}\,(\%) = \frac{P_N{}^{*}100}{\mathrm{RBC}_N} \tag{2}$$

where MC is the malaria parasites concentration in TBS, P_N is the number of parasites, WBC_N is the number of WBCs, MIR is the malaria infection rate in thin blood smear and RBC_N is the number of RBCs.

IV. Results and Discussion

Current studies on automated malaria detection have primarily focused on detecting malaria parasites, neglecting WBC count analysis. Furthermore, existing research has predominantly utilized high-quality image datasets and concentrated on WBC counts from thin blood smears, with limited investigation of TBS. Here, we address these gaps by training models using diverse datasets obtained through smartphone microscopy. We integrate clinical diagnostic methods for malaria with WBC counts on TBS to comprehensively assess a patient's condition. This approach facilitates the practical implementation and widespread adoption of this model in regions like Asia and Africa, where it is critically needed.

The aim of this study was to develop and validate an algorithm capable of automatically detecting malaria parasites and accurately counting WBCs in TBS. The proposed algorithm was designed and implemented using a comprehensive dataset obtained from the online National Institutes of Health (NIH) database. To ensure the model's applicability across diverse regions, a separate dataset from Sub-Saharan Africa (Sudan) was utilized. This approach enabled the evaluation of the algorithm's performance in a cross-regional context. In the subsequent section, we will provide a detailed assessment of the proposed model, including its accuracy, sensitivity, specificity, and other relevant performance metrics.

A. Performance of the Proposed Model on the NIH Dataset

1) Performance of the WBCs Classification Algorithm: We randomly selected 50 infected TBS and 50 uninfected TBS

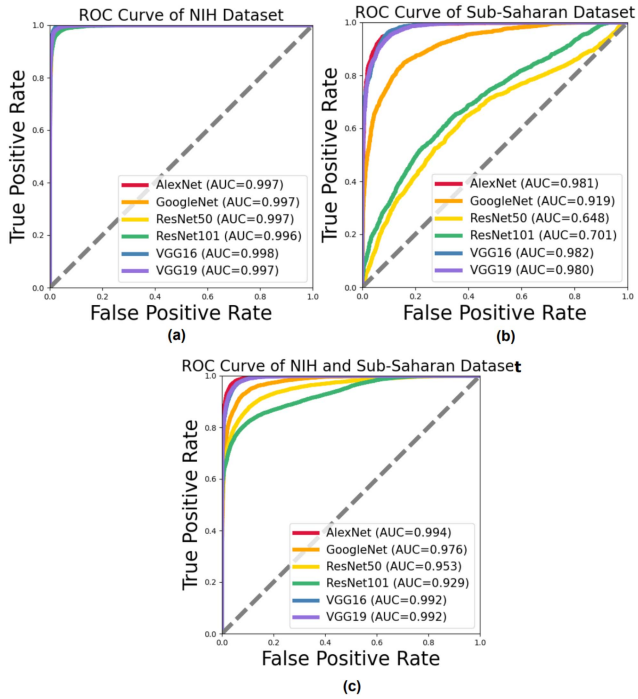

Fig. 7. ROC curve of each CNN architecture. (a) ROC curve of architectures trained by NIH dataset; (b) ROC curve of architectures trained by sub-saharan dataset; (c) ROC curve of architectures trained by mixed NIH and sub-saharan dataset.

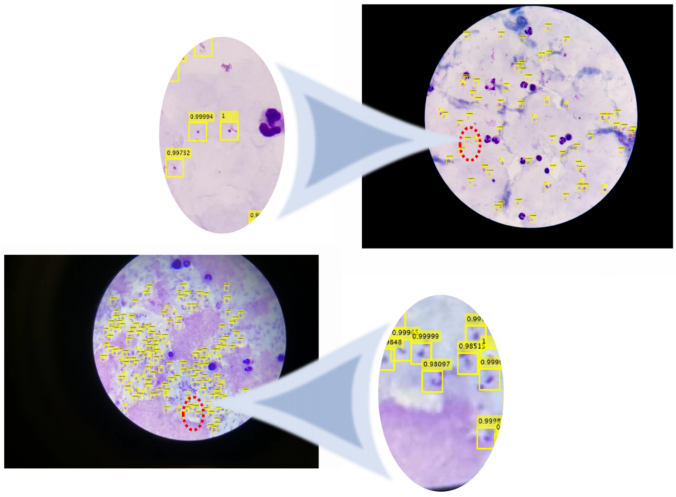

Fig. 8 *models-mix* model tests its results on both high-quality and low-quality datasets.

from the database. We used the proposed algorithm to perform the WBCs count on these 100 TBS. Subsequently, we compared the leukocyte counts obtained using only the Otsu algorithm and the combination of the Otsu algorithm with the *k*-means clustering algorithm. The experimental results showed that the correlation between the experimental value and the actual value was 98.7% and 98.9%, the mean absolute error (MAE) was 1.15 and 1.02, the mean square error (MSE) was 2.63 and 2.26, and the determination coefficient was 0.97 and 0.98, respectively. The result indicates that our WBCs count estimation achieves higher accuracy. Overall, the three comparative measures demonstrate the superiority of our proposed method over the Otsu algorithm. More detailed explanations are provided in Section II-A-1 of the Supplementary Materials.

2) Performance of the Malaria Detection Algorithm: Pre-trained VGG-16, VGG-19, AlexNet, GoogLeNet, ResNet-50, and ResNet-101 CNN models were considered for performance evaluation. The training parameters mentioned in the methodology section remained unchanged, and the NIH dataset consisted of 23,398 healthy images and 23,398 infected images. The CNN-based algorithms for malaria parasite detection, trained on the NIH dataset, are collectively referred to as *Models-NIH* onwards. The performance of these models on the NIH dataset is shown in Table 3 in the Supplementary Materials. VGG-19 model has shown the highest accuracy and F1-score, i.e., 97. 98 $\pm$ 0.13%, and 97.98 $\pm$ 0.1%, respectively.

B. Generalization of the Proposed Model Using the Sub-Saharan Africa Dataset

In this subsection, we present the performance evaluation of the malaria parasite detection algorithm using both the NIH dataset and the Sub-Saharan Africa dataset.

1) Model Performance. Training on the NIH Dataset, Testing on Sub-Saharan Africa Dataset: In this subsection, we evaluate the proposed model, which has been trained on the NIH dataset, the *Models-NIH*. The *Models-NIH* are tested using a dataset from Sudan. The aim of this investigation is to determine whether the online dataset collected solely from Asia is sufficient to generalize the proposed model.

Models trained using different datasets with their training results are detailed in Table 4 in the Supplementary Materials. All CNN models achieved a specificity above 99%; however, they yielded an accuracy of around 50%. The experimental results showed that the model trained on the NIH high-quality dataset had poor generalization ability on the low-quality dataset from Sudan and could not achieve accurate malaria parasite detection on the blurred images.

2) Assessing the Performance of a Mixed NIH and Sub-Saharan Dataset Trained Model. Testing on Sub-Saharan Data and NIH Data: To enhance the applicability of the model to low-quality image acquisition equipment in resource-limited areas, we integrated the Sudan dataset with the publicly available NIH dataset. The proposed model was trained on the combined dataset, which includes both the NIH and Sudan datasets. This training approach aimed to enhance the model's performance and generalization for cross-regional malaria detection. The CNN-based algorithms for malaria parasite detection, trained on the combination of Sudan and NIH datasets, are collectively referred to as *Models-Mix* onwards. The training parameters mentioned in the methodology section were kept unchanged, and the dataset comprised 33,517 healthy images and an equal number of 33,517 infected images.

The proposed model trained on a mixed dataset exhibits strong performance across the NIH dataset, Sudan dataset, and the mixed dataset. The performance of all CNN models is presented in Tables 5-7 in the Supplementary Materials. Among these

models, AlexNet consistently demonstrated the highest accuracy across all types of test sets, with an accuracy rate exceeding 92.44% and an F1-score of 92.18%. These results highlight the robustness and effectiveness of our proposed model, which is based on a mixed dataset. They underscore its generalization and high applicability in resource-limited areas.

Fig. 7 illustrates the Receiver Operating Characteristic (ROC) of each experiment, demonstrating the strong performance of each CNN architecture.

Fig. 8 illustrates the precise detection of malaria parasites in high-quality images from the NIH dataset as well as in low-quality images from the Sub-Saharan Africa dataset using the *Models-Mix*, AlexNet.

V. Conclusion and Future Work

In this paper, we have proposed an automatic malaria parasite detection algorithm for TBS. The results demonstrate that our proposed method can address the scarcity of medical personnel and equipment capable of producing only low-quality images in resource-poor regions like Africa. In this paper, we trained and validated the proposed model using a low-quality thin blood smear (TBS) dataset that includes novel malaria parasites, namely, falciparum and vivax parasites. This model is highly adaptable to malaria-endemic areas with limited medical resources. Additionally, we developed a fuzzy inference system to address the fuzzy regions caused by mismatched focal lengths between different types of mobile phone cameras and microscopes. Our method also has estimated the number of malaria parasites in the blood and counts WBCs to aid doctors in rapid diagnostic assessment of patients.

In summary, our proposed framework demonstrates high adaptability and significant potential for implementation in malaria-endemic regions. From a resource perspective, the smartphone microscope offers convenience and cost-effectiveness, making it suitable for resource-scarce scenarios in Africa. Moreover, when combined with deblurring algorithms, it addresses local image quality limitations associated with smartphone microscopy, enhancing its practicality. Additionally, our proposed detection model exhibits strong performance even on low-quality datasets, lowering entry barriers and conserving medical resources. From a user perspective, the white blood cell segmentation and counting algorithm assists doctors in identifying microscopic fields, saving reexamination time. Lastly, the designed GUI interface integrates all components, making it easier for medical professionals to access. Furthermore, the GUI interface enables real-time transmission of smartphone microscope images, facilitating intelligent microscopy.

The proposed malaria detection framework is specifically designed for application in regions prone to malaria, which often lack sufficient computing resources. When considering the tradeoff between accuracy and complexity, Google's Vision Transformer (ViT) demonstrates exceptional performance in our classification task [38]. ViT exhibits superior generalization capabilities compared to CNNs at equivalent complexity levels, making it more adept at handling limited data availability. Importantly, the proposed model surpasses existing methods, particularly in the analysis of low-quality images. This capability is crucial for aiding decision-making processes in underdeveloped countries with limited medical resources.

The limitations of the present study lie in the deblurring process of the image. To enhance the accuracy of malaria parasite detection, we sacrifice a portion of the field of view. However, this approach requires medical staff to identify additional fields of view to estimate the concentration of malaria parasites. In our future work, we plan to analyze additional types of malaria parasites, classifying various malaria parasite species in thick blood smears and exploring diverse deep transfer learning strategies. We will utilize public datasets and integrate a more substantial dataset from Sub-Saharan Africa to enhance accuracy. Additionally, our intention is to investigate algorithms for reconstructing and restoring blurred images, expanding beyond one-to-one image translation. This approach has the potential to decrease the requirement for extensive labeled data for each specific condition.

Supplementary Materials

The detailed processes and flowcharts for all the proposed algorithms, including defuzzification for captured microscope images and segmentation for WBCs, can be found in the Supplementary Materials. Additionally, the Supplementary Materials contain presentations of all performance metrics and comparisons related to malaria parasite detection based on DL.

Author Contributions

Conceptualization, S. S. M.; Data Analysis, Y. Z., Y. D., Y. C., J. L.; X. H. and O. M.; Methodology; Y. Z., Y. D., Y. C., J. L., O. M., E. S. H., A. K., S. S. M., and Q. F.; Supervision; S. S. M.; Funding acquisition, S. S. M., and Q. F. All authors participated in writing the paper.

Conflicts of Interest

The authors declare no conflict of interest.

Acknowledgment

The authors would like to thank the medical director and Dr. Ibrahim Alnnasri at Alkawa Hospital, Alkawa, White Nile State, Sudan, for approving the collection of the parasite images and the doctor at the Health Care Center of the First Affiliated Hospital of Shantou University, Yiteng Huang for providing blood smear to validate the efficiency of the proposed microscope.

References

[1] O. World Health, *World Malaria Report 2021*. Geneva, Switzerland: World Health Organization, 2021.

[2] C. W. Pirnstill and G. L. Coté, "Malaria diagnosis using a mobile phone polarized microscope," *Sci. Rep.*, vol. 5, no. 1, Aug. 2015, Art. no. 13368.

[3] L. Rosado, J. M. C. de Costa, D. Elias, and J. S. Cardoso, "Automated detection of malaria parasites on thick blood smears via mobile devices," *Procedia Comput. Sci.*, vol. 90, pp. 138–144, 2016.

[4] O. World Health, "WHO guidelines for malaria," World Health Organization, Geneva2023 2023, issue CC BY-NC-SA 3.0 IGO, Mar. 14, 2023. Accessed: Mar. 14, 2023. [Online]. Available: https://apps.who.int/iris/handle/10665/366432
[5] O. World Health, *Malaria Microscopy Quality Assurance Manual*, 2nd ed. Geneva, Switzerland: World Health Organization, 2016.
[6] R. Nakasi, E. Mwebaze, and A. Zawedde, "Mobile-aware deep learning algorithms for malaria parasites and white blood cells localization in thick blood smears," *Algorithms*, vol. 14, no. 1, 2021, Art. no. 17.
[7] M. Poostchi, K. Silamut, R. J. Maude, S. Jaeger, and G. Thoma, "Image analysis and machine learning for detecting malaria," *Transl. Res.*, vol. 194, pp. 36–55, Apr. 2018.
[8] A. Moody, "Rapid diagnostic tests for malaria parasites," *Clin. Microbiol. Rev.*, vol. 15, no. 1, pp. 66–78, 2002.
[9] A. H. Moody and P. L. Chiodini, "Methods for the detection of blood parasites," *Clin. Lab. Haematol.*, vol. 22, no. 4, pp. 189–201, Aug. 2000.
[10] E. Wynberg et al., "Variability in white blood cell count during uncomplicated malaria and implications for parasite density estimation: A worldwide antimalarial resistance network individual patient data meta-analysis," *Malaria J.*, vol. 22, no. 1, p. 174, Jun. 2023.
[11] A. Oliveira, M. Costa, M. Barbosa, and C. C. Filho, "A new approach for malaria diagnosis in thick blood smear images," *Biomed. Signal Process. Control*, vol. 78, Sep. 2022, Art. no. 103931.
[12] R. Liu et al., "AIDMAN: An AI-based object detection system for malaria diagnosis from smartphone thin-blood-smear images," *Patterns*, vol. 4, no. 9, Sep. 2023, Art. no. 100806.
[13] F. Yang et al., "Deep learning for smartphone-based malaria parasite detection in thick blood smears," *IEEE J. Biomed. Health Inform.*, vol. 24, no. 5, pp. 1427–1438, May 2020.
[14] P. Manescu et al., "Expert-level automated malaria diagnosis on routine blood films with deep neural networks," *Amer. J. Hematol.*, vol. 95, no. 8, pp. 883–891, Aug. 2020.
[15] F. Abdurahman, K. A. Fante, and M. Aliy, "Malaria parasite detection in thick blood smear microscopic images using modified YOLOV3 and YOLOV4 models," *BMC Bioinf.*, vol. 22, no. 1, Mar. 2021, Art. no. 112.
[16] K. Chakrabortya, A. Chattopadhyayb, A. Chakrabarti, T. Acharyad, and A. K. Dasguptae, "A combined algorithm for malaria detection from thick smear blood slides," *J. Health Med. Inform.*, vol. 6, pp. 1–6, 2015.
[17] D. K. Das, C. M. A. F. Chakraborty, and C. Chakraborty, "Automated system for characterization and classification of malaria-infected stages using light microscopic images of thin blood smears," *J. Microsc.*, vol. 257, no. 3, pp. 238–52, Mar. 2015, doi: 10.1111/jmi.12206.
[18] V. Acharya, V. Ravi, T. D. Pham, and C. Chakraborty, "Peripheral blood smear analysis using automated computer-aided diagnosis system to identify acute myeloid leukemia," *IEEE Trans. Eng. Manage.*, vol. 70, no. 8, pp. 2760–2773, Aug. 2023.
[19] P. Ghosh, D. Bhattacharjee, and M. Nasipuri, "Blood smear analyzer for white blood cell counting: A hybrid microscopic image analyzing technique," *Appl. Soft Comput.*, vol. 46, pp. 629–638, 2016.
[20] F. Olayah, E. M. Senan, I. A. Ahmed, and B. Awaji, "Blood slide image analysis to classify WBC types for prediction haematology based on a hybrid model of CNN and handcrafted features," *Diagnostics*, vol. 13, no. 11, 2023, Art. no. 1899.
[21] O. World Health, "Recording and reporting microscopy results," World Health Organization, Geneva2016, 2016. [Online]. Available: https://apps.who.int/iris/handle/10665/340461
[22] O. World Health, "Malaria parasite counting," World Health Organization, Geneva2016, 2016. [Online]. Available: https://iris.who.int/handle/10665/340469
[23] K. Al-Dulaimi, J. Banks, K. Nugyen, A. Al-Sabaawi, I. Tomeo-Reyes, and V. Chandran, "Segmentation of white blood cell, nucleus and cytoplasm in digital haematology microscope images: A review-challenges, current and future potential techniques," *IEEE Rev. Biomed. Eng.*, pp. 290–306, Jan. 2021, doi: 10.1109/RBME.2020.3004639.
[24] X. Zheng, Y. Wang, G. Wang, and J. Liu, "Fast and robust segmentation of white blood cell images by self-supervised learning," *Micron*, vol. 107, no. 8, pp. 55–71, Apr. 2018, doi: 10.1016/j.micron.2018.01.010.
[25] B. Kim, Y. Hariyani, Y. Cho, and C. Park, "Automated white blood cell counting in nailfold capillary using deep learning segmentation and video stabilization," *Sensors*, vol. 20, no. 24, Dec. 2020, doi: 10.3390/s20247101.
[26] S. Kaewkamnerd, C. Uthaipibull, A. Intarapanich, M. Pannarut, S. Chaotheing, and S. Tongsima, "An automatic device for detection and classification of malaria parasite species in thick blood film," *BMC Bioinf.*, 13, Dec. 2012, doi: 10.1186/1471-2105-13-S17-S18.
[27] M. Elter, E. Hasslmeyer, and T. Zerfass, "Detection of malaria parasites in thick blood films," *Annu. Int. Conf. IEEE Eng. Med. Biol. Soc.*, pp. 5140–5144, Aug. 2011, doi: 10.1109/IEMBS.2011.6091273.
[28] C. B. Delahunt et al., "Automated microscopy and machine learning for expert-level malaria field diagnosis," in *Proc. IEEE Glob. Humanitarian Technol. Conf.*, 2015, pp. 393–399.
[29] A. Vijayalakshmi and B. R. Kanna, "Deep learning approach to detect malaria from microscopic images," *Multimedia Tools Appl.*, vol. 79, no. 21/22, pp. 15297–15317, 2019.
[30] M. A.-O. Davidson et al., "Automated detection and staging of malaria parasites from cytological smears using convolutional neural networks," *Biol. Imag.*, Aug. 2021, doi: 10.1017/S2633903X21000015.
[31] C. Ikerionwu et al., "Application of machine and deep learning algorithms in optical microscopic detection of Plasmodium: A malaria diagnostic tool for the future," *Photodiagnosis Photodynamic Ther.*, 40:103198, Nov. 2022, doi: 10.1016/j.pdpdt.2022.103198.
[32] A. Kazarine, F. Baakdah, A. A. Gopal, W. Oyibo, E. Georges, and P. A.-O. Wiseman, "Malaria detection by third-harmonic generation image scanning cytometry," *Anal. Chem.*, vol. 91, no. 3, pp. 2216–2223, Jan. 2019, doi: 10.1021/acs.analchem.8b04791.
[33] M. Chacon, "Fuzzy logic for image processing: Definition and applications of a fuzzy image processing scheme," 2007.
[34] S. Sharma et al., "Image-based automatic segmentation of leaf using clustering algorithm," *Int. J. Nanotechnol.*, vol. 19, no. 6-11, pp. 539–553, 2022.
[35] T. Y. Goh, S. N. Basah, H. Yazid, M. J. A. Safar, and F. S. A. Saad, "Performance analysis of image thresholding: Otsu technique," *Measurement*, vol. 114, pp. 298–307, Jan. 2018.
[36] M. Alencastre-Miranda, R. M. Johnson, and H. I. Krebs, "Convolutional neural networks and transfer learning for quality inspection of different sugarcane varieties," *IEEE Trans. Ind. Informat.*, vol. 17, no. 2, pp. 787–794, Feb. 2021.
[37] W. Wang and Y. Yang, "Development of convolutional neural network and its application in image classification: A survey," *Proc. SPIE*, vol. 58, no. 4, 2019, Art. no. 040901.
[38] H. Wu et al., "CvT: Introducing convolutions to vision transformers," in *Proc. IEEE/CVF Int. Conf. Comput. Vis.*, 2021, pp. 22–31.